VISION ENHANCEMENT SYSTEM FOR DETECTION OF ORAL CAVITY NEOPLASIA BASED ON AUTOFLUORESCENCE

Ekaterina Svistun, MS,[1] Reza Alizadeh-Naderi, BS,[2] Adel El-Naggar, MD, PhD,[2] Rhonda Jacob, DDS,[2] Ann Gillenwater, MD,[2] Rebecca Richards-Kortum, PhD[1]

[1] Department of Biomedical Engineering, The University of Texas at Austin, Austin, Texas 78712.
E-mail: kortum@mail.utexas.edu
[2] Department of Head and Neck Surgery, The University of Texas M. D. Anderson Cancer Center, Houston, Texas

Accepted 25 August 2003
Published online 4 February 2004 in Wiley Interscience (www.interscience.wiley.com). DOI: 10.1002/hed.10381

Abstract: *Background.* Early detection of squamous cell carcinoma (SCC) in the oral cavity can improve survival. It is often difficult to distinguish neoplastic and benign lesions with standard white light illumination. We evaluated whether a technique that capitalizes on an alternative source of contrast, tissue autofluorescence, improves visual examination.

Methods. Autofluorescence of freshly resected oral tissue was observed visually and photographed at specific excitation/emission wavelength combinations optimized for response of the human visual system and tissue fluorescence properties. Perceived tumor margins were indicated for each wavelength combination. Punch biopsies were obtained from several sites from each specimen. Sensitivity and specificity were evaluated by correlating histopathologic diagnosis with visual impression.

Results. Best results were achieved with illumination at 400 nm and observation at 530 nm. Here, sensitivity and specificity were 91% and 86% in discrimination of normal tissue from neoplasia. This compares favorably with white light examination, in which sensitivity and specificity were 75% and 43%.

Conclusions. Oral cavity autofluorescence can be easily viewed by the human eye in real time. Visual examination of autofluorescence enhances perceived contrast between normal and neoplastic oral mucosa in fresh tissue resections. © 2004 Wiley Periodicals, Inc. *Head Neck* **26:** 205–215, 2004

Correspondence to: R. Richards-Kortum

Contract grant sponsor: Texas Higher Education Coordinating Board.

Keywords: oral cancer; squamous cell carcinoma; fluorescence imaging; detection

Five-year survival rates for patients with advanced squamous cell carcinoma (SCC) of the oral cavity are poor and have not improved significantly over the past 30 years.[1,2] Early detection of neoplastic changes in the oral cavity might be the best method to improve patient survival rates.[3–6] The current method of oral cancer diagnosis, visual examination of the oral cavity, relies heavily on clinical expertise in recognizing early neoplastic changes. However, discerning premalignant and early malignant lesions from common benign inflammatory conditions by visual examination can be difficult, even for experienced practitioners. Visual screening has been reported to have a sensitivity of only 74% and a specificity of 99%, and a positive and negative predictive value of 0.67 and 0.99, respectively.[7] Furthermore, both practitioners and patients are often reluctant to perform the invasive, sometimes painful biopsies that are required to confirm the presence of precancer or even early cancer.[8] Thus, despite the easy accessibility of the oral cavity to examination,

there is no satisfactory method to adequately screen and detect precancers noninvasively. Developing noninvasive and accurate techniques that can facilitate the early detection of neoplastic changes has great potential to improve survival rates and lower treatment costs in persons prone to have malignancies develop in the oral cavity.[3] There is a particular need for a simple, inexpensive, and objective screening method that can provide real-time results and be routinely applied to a large population.

Optical tools developed using knowledge of light and tissue interaction can provide such fast, noninvasive methods of cancer diagnosis. Normally, we observe reflected white light from objects, because this is the dominant light–tissue interaction. The conventional clinical method of oral cancer diagnosis relies on evaluation of tissue reflectance under illumination with white light. However, it is also possible to observe tissue autofluorescence, in which optical contrast between normal and neoplastic tissue might be significantly greater.[9–11]

When molecules within tissue absorb incident light, they may release energy in the form of fluorescent light.[12] The intensity and color of the fluorescence gives information about the local biochemical composition of tissue. Molecules capable of emitting light caused by optical excitation are called fluorophores. Autofluorescence originates from many endogenous fluorophores present in the tissue such as the crosslinks in the structural proteins collagen and elastin, the metabolic co-factors nicotinamide adenine dinucleotide (NADH) and flavin adenine dinucleotide (FAD^+), aromatic amino acids, such as tryptophan, tyrosine, and phenylalanine, and porphyrins.[8,12–15] Tissue fluorescence signatures are of particular interest, because spectral changes might reflect changes in metabolic activity and communication between the epithelium and the stroma.[16–18]

Several studies have previously explored whether spectroscopic or visual assessment of oral cavity autofluorescence properties can aid in oral cancer detection. It has been shown that spectroscopy of native oral fluorescence can discriminate between normal and neoplastic mucosa.[8,11,15,19–22] Fuchs[23] used a Woods lamp to illuminate the oral cavity tissue and then appraised the visually perceived differences. Bergenholtz and Welander[24] used a Hasselblad camera equipped with a set of filters for different excitation/emission conditions to record ultraviolet autofluorescence signal. Consistent trends in the observed photographed signal were reported from these studies. Onizawa et al[25] applied a custom photography system with built-in ultraviolet flash lamps exciting at 360 nm, and recorded autofluorescence greater than 480 nm achieved 88% sensitivity and 94% specificity in visually discriminating various oral cavity malignant conditions from the obtained images.

Although visual examination remains the mainstay for oral cancer diagnosis, our eyes are not optimized for the visual detection of neoplastic oral disease. Ordinarily, tissue fluorescence is not visible by eye, because it is masked by much more intense reflected light. However, by the use of spectral filters routinely used in fluorescence microscopy and flow cytometry that can block much of the reflected light,[13,19] oral autofluorescence can be perceived directly by the eye. Even so, the human eye can only extract a fraction of the existing chromatic information because of the physiologic properties of the color detection mechanisms.[26] The three types of cone photoreceptors have broadly overlapping spectral sensitivities, which might reduce the potential diagnostic contrast available when viewing tissue fluorescence. The excitation and illumination conditions used to image oral cavity fluorescence in previous studies were not optimized to enhance the differences in tissue fluorescence that can be perceived by the human visual system. In this article, we present our results obtained using an autofluorescence imaging system in which the illumination and observation conditions have been optimized to take into account the limitations of the human visual system.

Our approach to enhance visually perceived contrast involves optimization of illumination and fluorescence observation conditions by multispectral filtering of the excitation and emission light. This can be achieved in practice by exciting fluorescence with a fiberoptic illuminator and wearing a pair of filter glasses to observe tissue fluorescence. The selection of the excitation and observation filter combinations was governed by previous analyses performed in our laboratory. In two spectroscopic studies,[8,19] we measured the intensity of fluorescence of normal and neoplastic oral sites as a function of excitation and emission wavelength. In this work, we demonstrated that quantitative measurement of tissue fluorescence intensity could yield greater sensitivity and specificity relative to clinical examination, with best results at 350-, 380-, and 400-nm excitation.

Next, we asked the question, "In which spectral bands is the human eye most sensitive to differences between the normal and neoplastic tissue fluorescence signatures?" With the data from the spectroscopy studies and a model that predicts performance of a human observer in a color-discriminating task at the level of photoreceptors,[27] we predicted that optimal contrast would be achieved with excitation at 440 nm and observation between 500 and 560 nm (unpublished data).

This article describes the first prototype of a system constructed to excite and view fluorescence at these excitation and emission wavelengths. We evaluated the performance of this system in discriminating between normal and neoplastic lesions in oral cavity tissue resections. Our results demonstrate the feasibility of enhancing the perceived contrast between normal and neoplastic oral tissue with this approach, suggesting that simple, cost-effective devices that have potential to improve oral cavity cancer screening can be constructed.

MATERIALS AND METHODS

Instrumentation. Figure 1 shows a diagram of the system used to excite and view oral cavity fluorescence. The system consists of a light source filtered to provide optimal tissue illumination and a filter used to create optimal observation conditions. Fluorescence was viewed by eye and photographed using a standard 35-mm camera. The illumination is provided by a 300-watt Xenon ceramic short arc lamp with integrated parabolic reflector (Cermax, Perkin Elmer, Sunnyvale, CA). A cold mirror rejects radiation roughly below 300 nm and above 625 nm, preventing UV and infrared radiation from reaching the bandpass illumination filters. The cold mirror directs the collimated illumination beam into the filter wheel (Oriel Instruments, Stratford), which houses

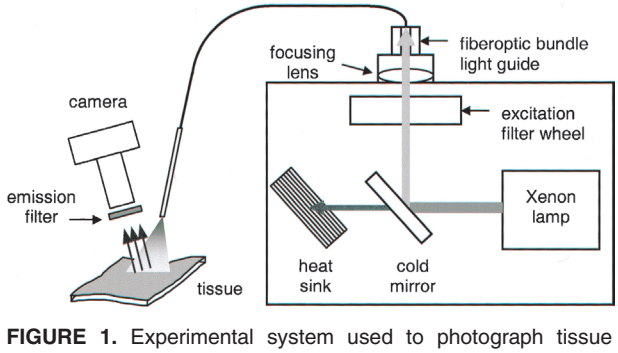

FIGURE 1. Experimental system used to photograph tissue fluorescence.

Table 1. Illumination conditions investigated for discrimination of normal and neoplastic oral cavity tissue flourescence.

Center wavelength, *nm*	Bandpass, *nm*
340	13
380	13
400	20
440	25

bandpass filters (Chroma Technology, Rockingham, VT). One of the filter wheel slots is left empty to provide white light illumination. Table 1 summarizes the filter specifications; the first three (350, 380, 400 nm) illumination conditions were selected on the basis of quantitative detailing of the entire emission spectrum, whereas the last (440 nm) was selected taking into account the performance of the human visual system.

The collimated beam passes through the filter box and is then focused onto a flexible fiberoptic bundle (Multimode Fiber Optics Inc, East Hanover, NJ), which can be used as a hand-held illuminator. The bundle is 5 mm in diameter and filled with 200-μm core diameter quartz fibers. The total length of the cable is 2.5 m. The system operator can guide the illuminating light in the entire oral cavity. The optimal operating distance is 20 to 30 cm, illuminating a surface from 4 to 8 cm in diameter.

Fluorescence was viewed through glasses containing a bandpass filter with maximum transmittance at 530 nm (60-nm bandwidth). To document tissue autofluorescence signal, a 35-mm SLR Canon EOS 630 camera was used to photograph fluorescence passing through the same bandpass filter. An EF 100-mm Canon macro lens was used for collection optics. The images were recorded on Kodak professional PORTRA 160 NC film, developed and printed professionally. The camera was fixed on a photographic copy stand above the imaged specimen. The distance between the camera lens and the specimen was adjusted so that the imaged resection filled the entire field of view. The three fluorescence images were photographed with 30 seconds exposure time and 2.8 f stop. The white light image was photographed at 1/350 second exposure time and 5.6 f stop.

Clinical Data. Four fresh tissue resections of a known or suspected premalignant or malignant oral cavity lesion were visualized and photographed after completion of frozen section

margin assessment and before processing the specimen for permanent pathologic analysis. The specimens were first rinsed with saline before multispectral imaging.

The fluorescence of each specimen was observed visually and then photographed with each of the four fluorescence illumination/observation conditions: 340, 380, 400, and 440 nm excitation, and 530 nm 60 BP observation, followed with a white light image. After tissue imaging, multiple 2- to 4-mm punch biopsies were performed and the specimens submitted for standard histopathologic diagnosis. The biopsy specimens were stained with a standard H & E protocol and read by a board-certified pathologist (AE) blinded to the results of the fluorescence images. The tissue was photographed again to record the punch biopsy sites for further analysis.

Data Processing. Each of the fluorescence and the white light images were evaluated by an experienced head and neck surgeon (AG), who was blinded to the histopathologic diagnosis of the punch biopsy specimens. Suspected neoplastic areas on printed photographic images were encircled. Punch biopsy sites were then overlaid on top of the images with drawn margins, and the

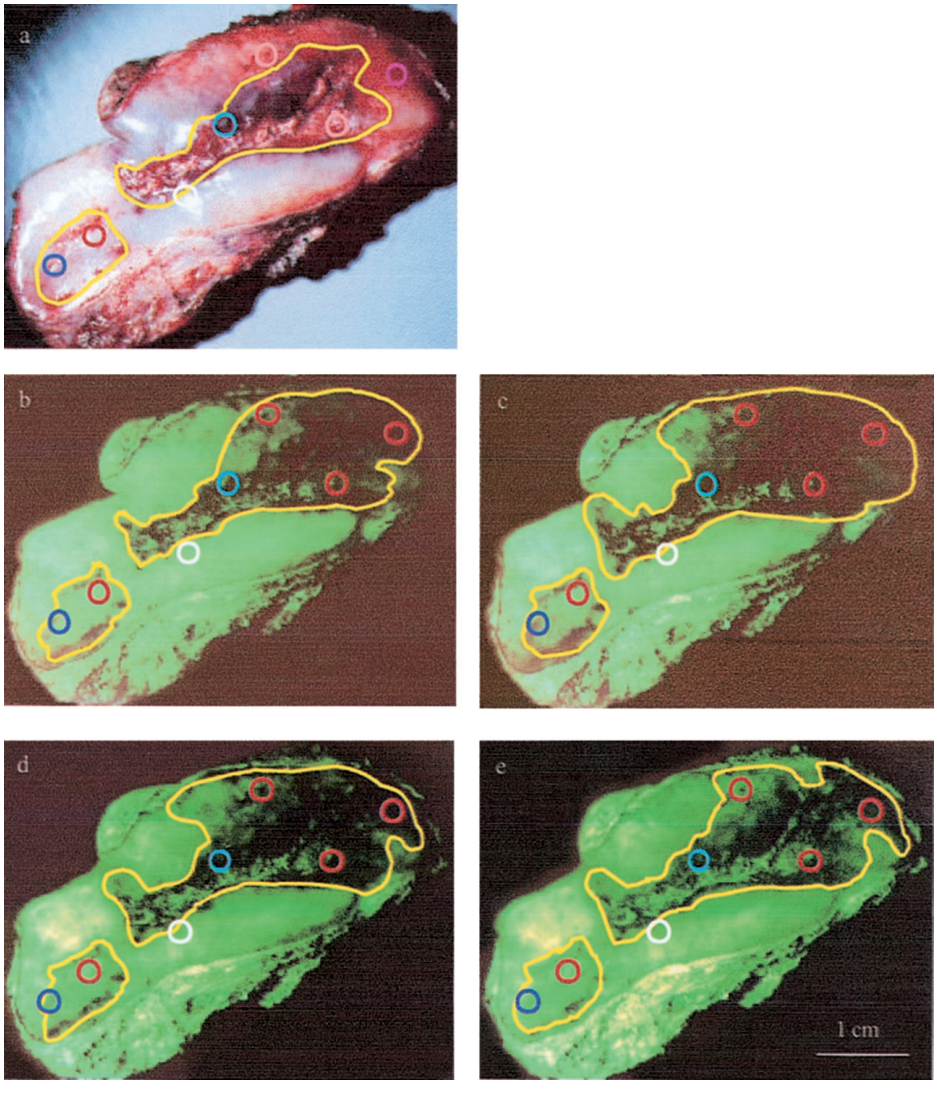

FIGURE 2. White light (a) and autofluorescence images obtained from patient 1—invasive cancer of the buccal mucosa of the cheek. Image is photographed with excitation (b) at 340 nm, (c) at 380 nm, (d) at 400 nm, and (e) at 440 nm. Yellow lines encircle the suspected tumor margins specified by the clinician. Punch biopsies sites are color coded according to their histopathologic diagnosis: white represents normal tissue, blue represents dysplasia, and red represents squamous cell carcinoma.

diagnosing ability of each observation condition was evaluated relative to histopathologic diagnosis. Abnormal biopsy sites accurately detected and encircled within the tumor margin area were counted as true positives, and those left undetected outside the tumor margin were considered as false negatives. The normal biopsy sites accurately discriminated from the neoplastic suspicious areas were counted as true negatives, and those that were encircled within the tumor margin area were counted as false positives. Two definitions of abnormal tissue were used; in the first, only biopsy specimens showing cancer were counted as abnormal, and in the second, biopsy specimens showing either cancer or dysplasia were included as abnormal.

RESULTS

Four oral cavity resection specimens were evaluated: one severe dysplasia of the tongue, one mild dysplasia of the tongue, one invasive SCC of the buccal mucosa, and an invasive SCC of the floor of mouth. In all cases, autofluorescence was easily visible by the eye and yellow-green in color. Figures 2 through 5 show a white light photo-

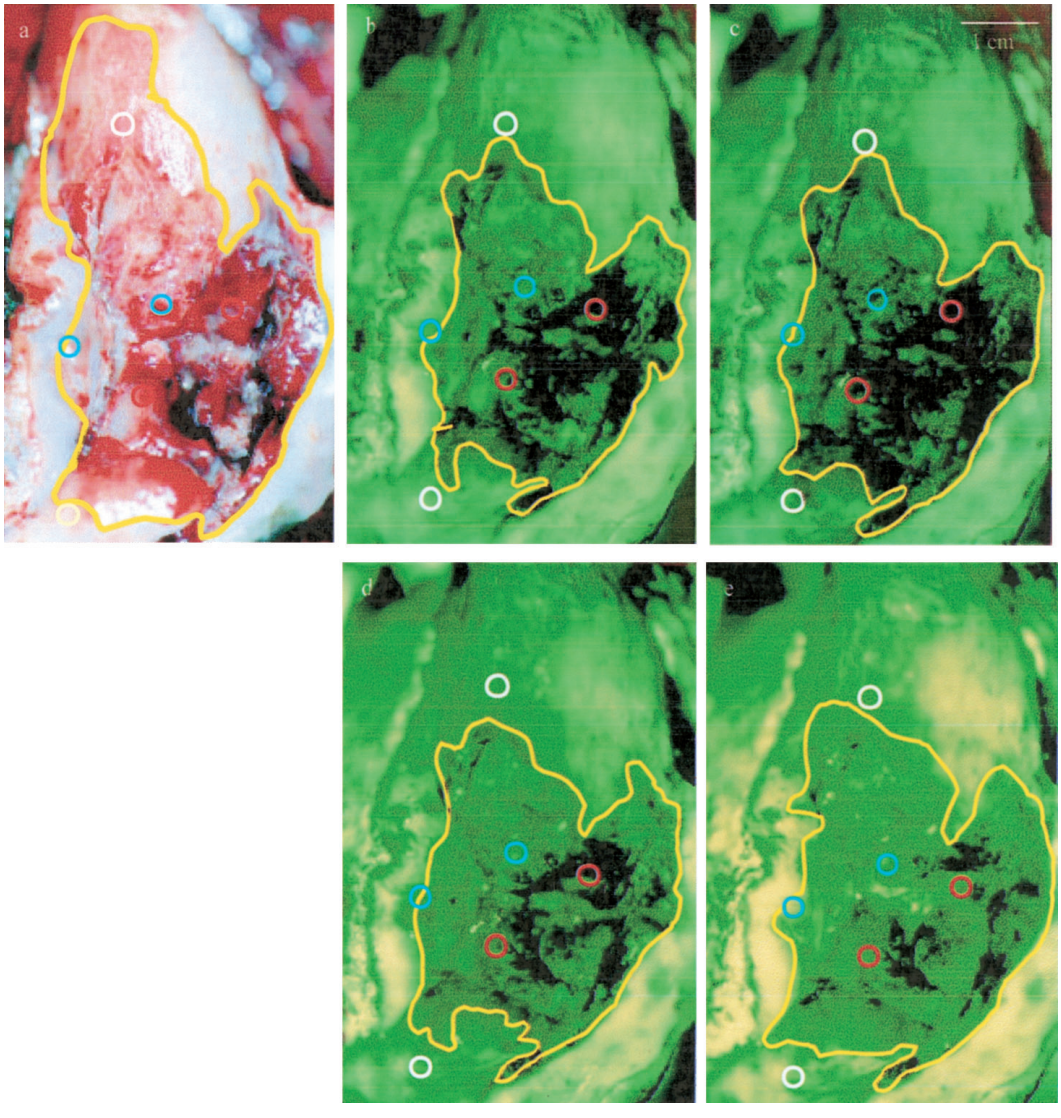

FIGURE 3. White light (a) and autoflourescence images obtained from patient 2—invasive cancer on the floor of mouth. Image is photographed with excitation (b) at 340 nm, (c) at 380 nm, (d) at 400 nm, and (e) at 440 nm. Yellow lines on the images encircle the suspected tumor margins specified by the clinician. Punch biopsies sites are color coded according to their histopathologic diagnosis: white represents normal tissue, blue represents dysplasia, and red represents squamous cell carcinoma.

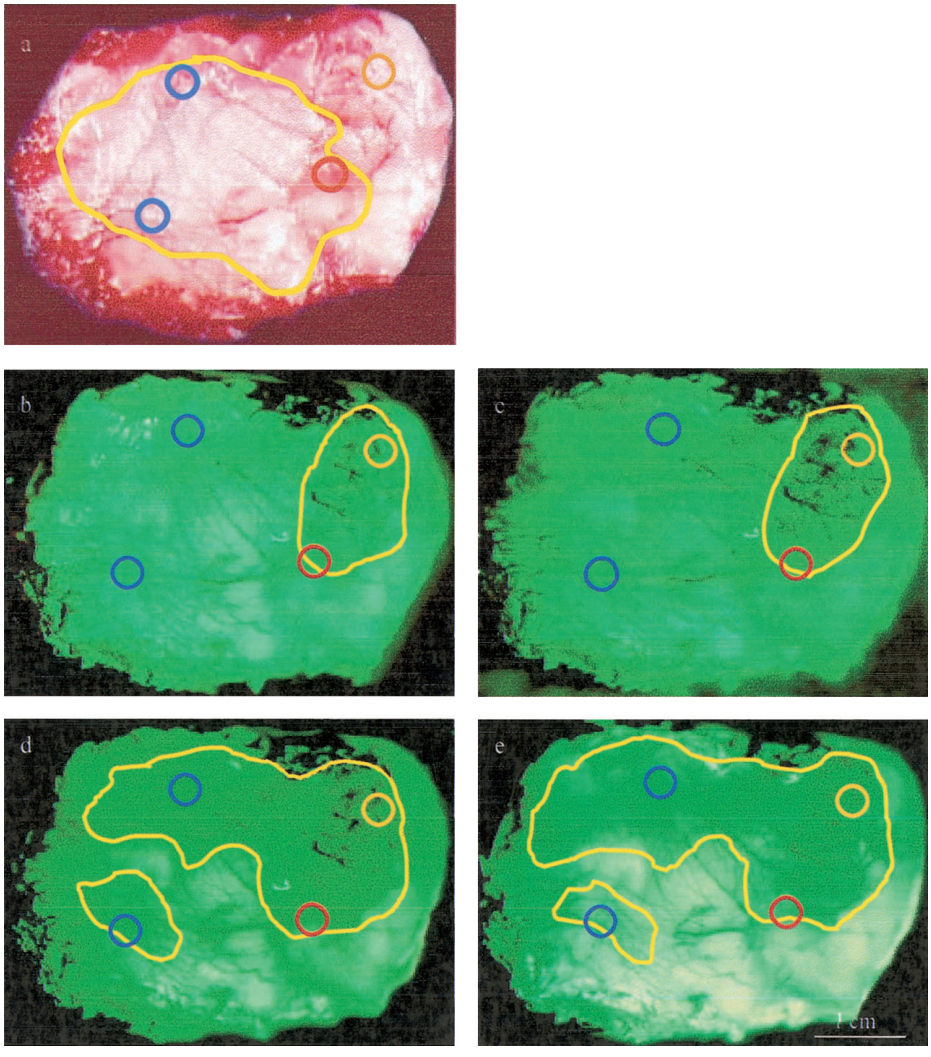

FIGURE 4. White light (a) and autoflourescence images obtained from patient 3—visually diagnosed as severe dysplasia of the tongue. Image is photographed with excitation (b) at 340 nm, (c) at 380 nm, (d) at 400 nm, and (e) at 440 nm. Yellow lines on the images encircle the suspected tumor margins specified by the clinician. Punch biopsies sites are color coded according to their histopathologic diagnosis: blue represents dysplasia, orange represents carcinoma in situ, and red represents squamous cell carcinoma.

graph and autofluorescence images of all resected specimens. In each image, yellow lines encircle the suspected tumor margins, and the punch biopsy sites are overlaid. The punch biopsy sites are coded according to the histopathologic diagnosis: solid white represents normal tissue, blue represents dysplasia, orange represents carcinoma in situ, and dashed white represents cancer.

Figure 2 shows the white light image and four fluorescence images obtained from the buccal mucosa resection. Seven punch biopsy specimens were obtained. The fluorescence images show a bright green fluorescent area with two regions of lower intensity that appear dark. The evaluating clinician highlighted these two regions as the suspicious cancerous areas. The corresponding white light reflectance image presents with much more color and textural detail. It is easy to discern the raised lesion in the center. There is also noticeable erythroplakia in the upper right hand corner of the image; however, its margins are not defined, and the clinician included only a portion of that area in the suspected tumor margin. It is readily appreciated that using the four fluorescence imaging modes neoplastic areas could be identified with greater sensitivity. Both the dysplastic and the cancerous sites were detected accurately and discriminated from normal tissue. However, standard white light reflectance examination missed two cancerous sites.

Figure 3 shows the white light image and four fluorescence images obtained from the resection

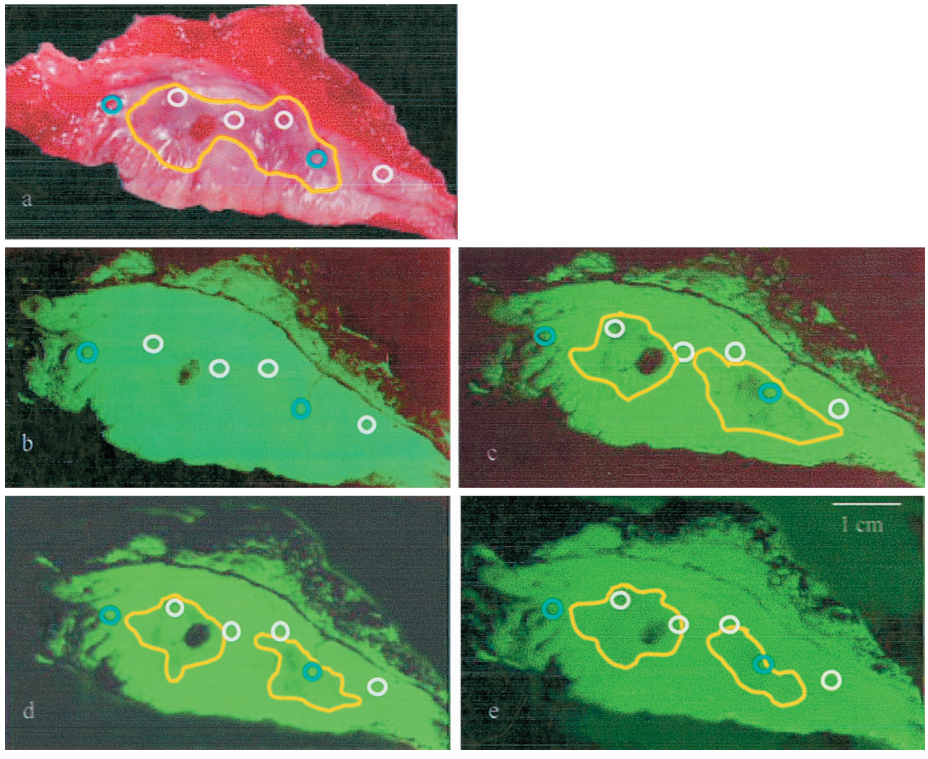

FIGURE 5. White light (a) and autoflourescence images obtained from patient 4—mild dysplasia of the tongue. Image is photographed with excitation (b) at 340 nm, (c) at 380 nm, (d) at 400 nm, and (e) at 440 nm. Yellow lines on the images encircle the suspected tumor margins specified by the clinician. Punch biopsies sites are color coded according to their pathologic diagnosis: white represents normal tissue and blue represents dysplasia.

from the floor of the mouth. The white light reflectance view of the tumor resection presents many details: speckled red and white areas, many topographic features, and areas of tissue necrosis. The autofluorescence images of this tissue resection again show a green autofluorescence with a central darker region. The suspected tumor margins drawn on all the fluorescence images encircled these areas of lower intensity, which encompassed a slightly smaller area than that of the corresponding white light image tumor margin. Five punch biopsy specimens were obtained; the overlaid punch biopsy sites reveal that the autofluorescence observation technique achieved greater specificity. One dysplastic biopsy site fell on the specified tumor margin in two fluorescence images excited at 380 and 440 nm and was falsely identified as negative with 340-nm excitation.

Figure 4 shows the white light image and four fluorescence images obtained from the resection of a tongue lesion with severe dysplasia. The white light reflectance image of this resection presents minimal detail. The fluorescence images show lower intensity at the upper right hand area of the images with 340- and 380-nm excitation, and extended lower intensity areas spanning the upper half of the 400- and 440-nm excitation images. Four punch biopsy specimens were obtained. The biopsy results showed that white light reflectance observation failed to detect the region identified as carcinoma in situ, whereas all four fluorescence images detected it accurately. Exciting at both 340 and 380 nm, two dysplastic sites were not discerned from the surrounding normal tissue, and the biopsy site diagnosed as SCC fell on the drawn tumor margin. However, exciting at 400 and 440 nm, all the abnormal areas were diagnosed accurately.

Figure 5 shows the white light image and four fluorescence images obtained from a tongue resection for mild dysplasia. In the white light reflectance image, a slightly darker center area was encircled as the suspected lesion. In three autofluorescence images (excited at 380, 400 and 440 nm) two central dark areas are visible against the bright green background. However, excitation at 340 nm did not yield any perceivable contrast. Six punch biopsy specimens were obtained. All the imaging methods missed one dysplastic site. Nonetheless, three fluorescence images were able

Table 2. Summary of tumor and biopsy sites for the patient set.

	Tumor location	Number of biopsies	Normal	Dysplasia	CIS	SCC
Patient 1	Buccal mucosa	7	1	2		4
Patient 2	Floor of mouth	6	2	2		2
Patient 3	Tongue, superior	4		2	1	1
Patient 4	Tongue, inferior	6	4	2		
	Total:	23	7	8	1	7
	Presence of inflammation	13	3	6	1	3

Abbreviations: CIS, carcinoma in situ, SCC, squamous cell carcinoma.
Inflammation grade varied from mild to severe.

to discriminate normal sites with higher specificity than with white light reflectance observation.

The results of histopathologic analysis of the biopsy specimens and their distribution are summarized in Table 2. Of the 23 biopsy specimens, seven were normal, eight dysplastic, and eight malignant. Normal pathology included hyperkeratosis, hyperplasia, and inflammation. The eight dysplasias ranged from mild to severe. One malignant biopsy was a carcinoma in situ (CIS), and seven were invasive SCCs. In all the further analyses, CIS was grouped with SCC and considered as cancer. Of the seven normal biopsy specimens, three showed the presence of inflammation on histologic examination. Six of the eight dysplasias, the one CIS, and three of the seven SCCs had inflammation, and the inflammation grade varied from mild to severe.

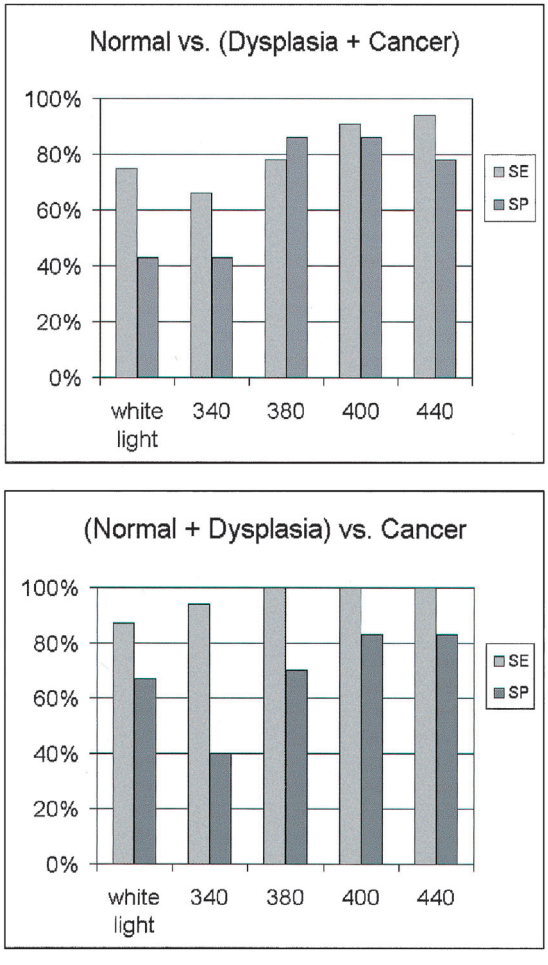

FIGURE 6. Top: Sensitivity and specificity for discriminating normal tissue from dysplasia and cancer based on white light and fluorescence images. Bottom: Sensitivity and specifity for discriminating cancer from normal tissue and dysplasia using white light and fluorescence images.

The sensitivity and specificity of each illumination/observation condition were calculated on the basis of agreement between the visually perceived tumor margins and histopathologic findings for the 23 biopsied sites. Results are summarized in Figure 6. Initially, sensitivity and specificity were calculated grouping dysplasia and cancer together as diseased (Figure 6a). Subsequently, sensitivity and specificity were evaluated when discriminating cancer from normal and dysplastic sites together (Figure 6b).

Three of the four different fluorescence illumination/observation conditions yielded higher sensitivity and specificity compared with white light examination. Under white light illumination, sensitivity for cancer detection was 87% and specificity was 67%; for detection of dysplasia and cancer together, sensitivity was 75% and specificity was only 43%. The best results were achieved with illumination at 400 and 440 nm, where sensitivity and specificity for detection of cancer were 100% and 83% at both wavelengths. For detection of dysplasia and cancer together, sensitivity and specificity were 91% and 86% at 400-nm excitation and 94% and 78% at 440-nm excitation.

DISCUSSION

Fluorescence images obtained with the vision enhancement system consistently revealed lower intensity autofluorescence signal from the neo-

plastic oral cavity sites. This observation is consistent with the findings obtained by our group[19,28] and others,[14,20–22,29,30] where dysplastic and cancerous emission spectra presented with overall lower signal intensity than normal tissue.

The best sensitivity and specificity were achieved when fluorescence was observed with a 60-nm spectral band centered at 530 nm with excitation at either 400 or 440 nm. These optimal excitation wavelengths correlate with the findings by Heintzelman et al[19] from quantitative evaluation of spectroscopically collected data and from an analysis of the performance of the human visual system. The least favorable results were achieved at 340-nm excitation. The task of discriminating cancer from normal and dysplastic sites yields much higher sensitivity and specificity for all the fluorescence images and white light illumination compared with the task of discerning dysplasia from normal oral mucosa. This finding correlates with the diagnostic observation: dysplastic lesions are more difficult to identify in the oral cavity and are often similar in appearance to normal tissue. Although we evaluated only a small number of specimens, the presence or absence of inflammation did not seem to affect our ability to use fluorescence images to discriminate between the normal and neoplastic tissues.

The exact mechanisms underlying alteration in epithelial autofluorescence with malignant progression remain unclear. The overall optical signal that can be detected is determined by the relative quantities and distribution of tissue fluorophores that fluoresce and chromophores that absorb or scatter light. Fluorophores that are likely to contribute strongly to autofluorescence of oral tissue include collagen cross-links, reduced NADH, oxidized FAD, and amino acids such as tryptophan.[13,14]

With excitation at 400 nm, it is possible that the decrease in fluorescence intensity in the abnormal sites of tissue resections is also due to hemoglobin absorption. Hemoglobin absorbs strongly at 420 nm.[14] Tumors are associated with angiogenesis leading to progressively increased microvessel density[31–33]; the increase in blood volume might result in reduced autofluorescence signal. Also, collagen cross-link decomposition, associated with neoplasia development,[18] contributes to the reduction of fluorescence signal intensity. Müller et al[21] have shown that oral cavity carcinoma is accompanied by an increase in epithelial thickness, which reduces the depth of penetration of excitation light that reaches stromal collagen, thus reducing its contribution to the total signal.

An important limitation to this study is that it was performed using ex vivo specimens. The possible contributions to the optical signal from metabolic cofactors NADH and FAD, collagen cross-links, and hemoglobin might be affected when tissue is resected, and the optimal activation wavelengths in vivo might differ from those determined on excised tissue. Schomaker et al[30] have demonstrated that NADH present in the tissue is oxidized to NAD^+ in anaerobic conditions initiated by tissue excision, and fluorescence from this metabolic cofactor decreases exponentially within 2 hours after the resection. To minimize this effect, we imaged the tissue immediately after excision, with the maximum time elapsed not exceeding 1 hour, minimally affecting tissue viability. However, our findings will need to be confirmed through inspection of oral lesions in vivo using this system. Nevertheless, our results demonstrate proof of the concept of enhancing the ability of clinicians to visualize neoplastic oral tissue using defined wavelengths to visualize native tissue autofluorescence.

When identifying tumor margins on the white light images, the physician was guided by visual cues learned from training and experience in oral cavity cancer diagnosis. When analyzing the autofluorescence images, she did not have any previously developed skills in recognition. The results presented here, although based on a small sample size, demonstrate that the proposed autofluorescence imaging technique might provide better sensitivity and specificity than standard white light examination, even when a clinician having no experience in evaluation of fluorescence images performs such diagnosis. This suggests that the vision-enhancement technique has the potential to improve oral cavity cancer diagnosis for even inexperienced practitioners.

This visualization system provides a technique with potential to analyze the entire epithelial surface rapidly and noninvasively, while retaining cues already used by clinicians in oral cavity cancer diagnosis and sharpening the perceived contrast between normal and abnormal mucosa with optimized spectral filtering. Noninvasive, rapid, cost-effective, and simple devices can be constructed on the basis of the concept of enhanced visualization. Such a vision enhancement system not only can be used as a diagnosing tool but also can aid in tumor margin determination during surgery. Enhanced visualization

tools can also be used to guide high-resolution imaging devices such as in vivo confocal microscopy and optical coherence tomography (OCT). These endoscopic microscopes can provide high-resolution images of cellular morphology and tissue architecture from a small field of view (< 500 μm). Without appropriate guidance to select suspicious fields to image with high magnification, confocal microscopy and OCT would be ineffective for entire oral cavity screening. With appropriate guidance from the simple autofluorescence imaging presented here, endoscopic microscopes would be rendered more effective in their application for localized diagnosis.

This visualization system will need to be tested and refined in both an office and an operative setting to determine whether our observations on resected specimens will correlate with the findings in vivo. A prospective clinical trial is being initiated to evaluate this important point. In addition, it will be important to evaluate and compare the autofluorescence that can be detected from cancerous, dysplastic, and inflammatory tissue to determine how well the physicians can distinguish between these entities using selected illumination conditions and white light. The results presented here are an important step in this development process, because they provide proof of concept to support future in vivo trials.

The presented system was developed for diagnosis of oral cavity cancer; however, one can extend the same principle to cancer diagnosis in other sites where visual examination is possible, such as laryngoscopy, bronchoscopy, colposcopy of the cervix, or endoscopic colonoscopy. This represents an enormous opportunity to develop simple, inexpensive, but accurate, devices that capitalize on these findings.

REFERENCES

1. American Cancer Society. http://www.cancer.org.
2. Blair EA, Callendar DL. Head and neck cancer—the problem. Clin Plast Surg 1994;21:1–7.
3. Gillenwater A, Jacob R, Richards-Kortum R. Fluorescence spectroscopy: a technique with potential to improve the early detection of aerodigestive tract neoplasia. Head Neck 1998;20:556–562.
4. U.S. Department of Health and Human Services, Centers for Disease Control and Prevention. The National Breast and Cervical Early Detection Program. Atlanta: Centers for Disease Control and Prevention; 2001.
5. U.S. Department of Health and Human Services, Centers for Disease Control and Prevention. Improving Oral Health: Preventing Unnecessary Disease Among All Americans. Atlanta: Centers for Disease Control and Prevention; 2001.
6. U.S. Department of Health and Human Services, Centers for Disease Control and Prevention. Colorectal Cancer: The Importance of Prevention and Early Detection. Atlanta: Centers for Disease Control and Prevention; 2001.
7. Jullien JA, Downer MC, Zakrzewska JM, Speight PM. Evaluation of a screening test for the early detection of oral cancer and precancer. Community Dent Health 1995;12:3–7.
8. Gillenwater A, Jacob R, Ganeshappa R, et al. Noninvasive diagnosis of oral neoplasia based on fluorescence spectroscopy and native tissue autofluorescence. Arch Otolaryngol Head Neck Surg 1998;124:1251–1258.
9. Harries ML, Lam S, MacAulay C, Qu J, Palcic B. Diagnostic imaging of the larynx: autofluorescence of laryngeal tumours using the helium-cadmium laser. J Laryngol Otol 1995;109:108–118.
10. Palcic B. Endoscopic imaging system for diseased tissue (United States patent number 5,507,287, 1996).
11. Betz C, Mehlmann M, Rick K, et al. Autofluorescence imaging and spectroscopy of normal and malignant mucosa in patients with head and neck cancer. Lasers Surg Med 1999;25:323–334.
12. Lakowicz JR. Principles of fluorescence spectroscopy, 2nd ed., New York: Plenum Publishers; 1999.
13. Wagnieres GA, Star WM, Wilson BC. In vivo fluorescence spectroscopy and imaging for oncological applications. Photochem Photobiol 1998;68:603–632.
14. Richards-Kortum RR, Sevick-Muraca E. Quantitative optical spectroscopy for tissue diagnosis. Annu Rev Phys Chem 1996;47:555–606.
15. Ramanujam N. Fluorescence spectroscopy of neoplastic and non-neoplastic tissues. Neoplasia 2000;2:89–117.
16. Sokolov K, Galvan J, Myakov A, Lacy A, Lotan R, Richards-Kortum RR. Realistic three-dimensional epithelial tissue phantoms for biomedical optics. J Biomed Opt 7: 148–156.
17. Drezek R, Brookner C, Pavlova I, et al. Autofluorescence microscopy of fresh cervical-tissue sections reveals alterations in tissue biochemistry with dysplasia. Photochem Photobiol 2001;73:636–641.
18. Brookner C, Follen M, Boiko I, et al. Autofluorescence patterns in short-term cultures of normal cervical tissue. Photochem Photobiol 2000;71:730–736.
19. Heintzelman D, Utzinger U, Fuchs H, et al. Optimal excitation wavelengths for In vivo Detection of oral neoplasia using fluorescence spectroscopy. Photochem Photobiol 2000;72:103–113.
20. Schantz SP, Koli V, Savage HE, et al. In vivo native cellular fluorescence and histological characteristics of head and neck cancer. Clin Cancer Res 1998;4:1177–1182.
21. Müller MG, Valdez TA, Georgakoudi I, et al. Spectroscopic detection and evaluation of morphologic and biochemical changes in early human oral carcinoma. Cancer 2003;97:1681–1692.
22. Andersson-Engels S, Klinteberg C, Svanberg S. In vivo fluorescence imaging for tissue diagnostics. Phys Med Biol 1997;42:815–824.
23. Fuchs M. Überdie Fluoreszenz der Mundhöhle und der Zöhne. Schweizerische Monatsschritt für Zahnheikunde. 69:1959.
24. Bergenholtz A, Welander U. Ultraviolet autofluorescence: an aid in oral diagnosis. Dent Radiogr Photogr 1970; 43:83–89.
25. Onizawa K, Saginoya H, Furuya Y, Yoshida H. Fluorescence photography as a diagnostic method for oral cancer. Cancer Lett 1996;108:61–66.
26. Wandell B. Foundation of vision. Sunderland, MA: Sinauer Associates; 1995.
27. Utzinger U, Bueeler M, Oh S, et al. Optimal visual

perception and detection of oral cavity neoplasia. IEEE Trans Biomed Eng 2003;50:396–399.
28. Zuluaga A, Utzinger U, Durkin A, et al. Fluorescence excitation emission matrices of human tissue: a system for in vivo measurement and method of data analysis. Appl Spectrosc 1999;53:302–311.
29. Katz A, Savage HE, Schantz SP, McCormick SA, Alfano RR. Noninvasive native fluorescence imaging of head and neck tumors. Technol Cancer Res Treat 1:9–15.
30. Schomacker KT, Frisoli JK, Compton CC, et al. Ultra-violet laser-induced fluorescence of colonic tissue: basic biology and diagnostic potential. Lasers Surg Med 1992;12:63–78.
31. Dobbs SP, Hewett PW, Johnson IR, Carmichael J, Murray JC. Angiogenesis is associated with vascular endothelial growth factor expression in cervical intraepithelial neoplasia. Br J Cancer 1997;76:1410–1415.
32. Dellas A, Moch H, Schultheiss E, et al. Angiogenesis in cervical neoplasia: microvessel quantitation in precancerous lesions and invasive carcinomas with clinicopathological correlations. Gynecol Oncol 1997;67:27–33.
33. Obermair A, Bancher-Todesca D, Bilgi S, et al. Correlation of vascular endothelial growth factor expression and microvessel density. J Natl Cancer Inst 1997;89: 1212–1217.